

AN INJECTOR COMPONENT MODEL FOR COMPLETE MICROFLUIDIC ELECTROKINETIC SEPARATION SYSTEMS

R. Magargle^{*}, J.F. Hoburg^{**} and T. Mukherjee^{***}

Carnegie Mellon University, Pittsburgh, PA 15213, USA

*magargle@cmu.edu, **hoburg@ece.cmu.edu, ***tamal@ece.cmu.edu

ABSTRACT

This work presents a closed-form, numerically derived model of a key microfluidic electrokinetic separation system component, the cross injector. The model fits into a framework such that it can be combined with a network of other component models, such as a mixer, reactor, separation channel, and detector, to model a complete microfluidic separation system. The model is based on a reduction of the full 5-dimensional parameter space to a manageable 2-dimensional parameter space. The resultant model is valid for Peclet numbers ranging from 10 to 5000 and shows a worst case variance equal to the channel width squared.

Keywords: microfluidic, electrokinetic, cross, injector

1 INTRODUCTION

The injector is a very important component of the microfluidic separation system since it defines the shape and quantity of analyte that will be used for separation and analysis. Much work has been done previously to describe the various forms of microfluidic electrokinetic injectors, such as the tee, double-tee, cross, and double-cross [1-5]. This work presents a new form of the cross injector model that is compatible with a system network of component models, [6,7]. In 2000, Ermakov, et al., extensively modeled the effects of field ratios on the injected band for a cross injector [5]. The metrics used to measure the performance of the injector were based on the maximum concentration and the standard deviation of the transversely averaged concentration profile. The component injector model in this paper is based on similar metrics and uses similar notations to those in [5].

The methodology described here involves an exploration of a relevant portion of the injector parameter space using finite element, partial differential equation solutions of the convection diffusion equation. The local electrokinetic velocity is proportional to the local electric field. These solutions are then used to create fitted expressions for the desired input-output values, which are the input species concentration and the resulting output variance and maximum concentration. The output parameters are sufficient to construct a Gaussian distribution, approximating the width averaged plug

concentrations as a function of longitudinal position, for the input to the separation channel.

2 INJECTOR DESIGN

A 2-stage cross injector with accessory fields is shown in Figure 1. The accessory fields in the loading stage confine the band within the injection chamber, reducing the variance of the band, and they provide temporal stability for analytes with components of varying mobilities. These loading stage accessory fields are also known as pinching fields and were recommended for use in cross topologies nearly a decade ago [1]. The accessory fields used in the dispensing stage pull the band out of the injection chamber to ensure a clean exit. The two-stage cross injector is a commonly implemented design due to its relative simplicity and good performance.

Some alternative injector topologies and control schemes are summarized in Table 1. This table provides a qualitative measure of the performance of each injector with regard to output band variance, maximum concentration, and uniformity of the band shape. It also gives an indication of the control complexity by listing the number of voltage control stages that are typically used for each injector type. The cross injector also sometimes employs 3-stage voltage control schemes. These include, the gated cross injection scheme [5] and a variation of the 2-stage injection that adds a pullback step before the dispensing stage [4]. Table 1 shows a qualitative assessment of the popularity of each topology in its final

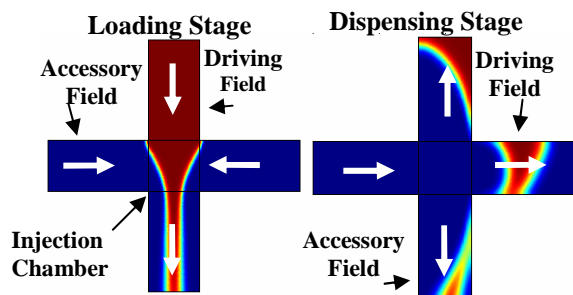


Figure 1 – The two stage cross injector. In the loading stage, the accessory electric fields horizontally pinch the analyte as it is driven vertically downward by the driving electric field. In the dispensing stage, the accessory electric fields vertically pull the analyte away from the intersection while the driving fields horizontally drive the plug into the separation channel.

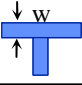
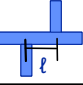
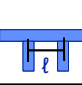
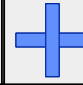
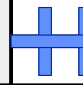
					
Injector Type	Tee	Double Tee	Pi	Cross	Double Cross
Common Injection Schemes	2 stage	2 stage	2 stage 3+ stage	2 stage 3+ stage	2 stage
σ^2	$> w^2$	$\sim \ell^2$	$\sim \ell^2$	$< w^2$	$< w^2$
C_{max}	H	H	H	M	M
Plug Uniformity	L	H	M	MH	H
Popularity	LM	MH	L	H	M

Table 1 – Injector topologies and control schemes. L, M, H refer to low, medium, high. w is the channel width, and ℓ is a channel separation length.

row, based upon instances of use in typical designs. Since the cross injector with 2-stage accessory fields combines a simple and popular topology with a reduced control scheme that is capable of good performance, it is pursued in detail here for incorporation into a component network model.

3 PROBLEM SPACE

The first step in the modeling procedure is identification of a complete set of non-dimensional variables that parameterize the problem space based on the known physical variables of the system. The physical variables governing the dynamics of the cross injector are summarized in Table 2(a,b), where μ is the electrokinetic mobility, κ is the species diffusivity, w_L is the width of the loading channels, w_D is the width of the dispensing channels, E_{iL} and E_{iD} represent the electric field at the injector inlet in the i th leg for the loading, L , and dispensing stages, D , respectively as shown in Figure 2.

The non-dimensional variables in Table 2(c) are

Loading Stage Variables – (a)		
Species	Geometry	Stimuli
μ	w_L	$E_{2,4L}$
κ	w_D	E_{1L}
Dispensing Stage Variables – (b)		
Species	Geometry	Stimuli
μ	w_L	E_{2D}
κ	w_D	$E_{1,3D}$
Non-Dimensionalized Variables – (c)		
$\omega = w_L/w_D$	$\epsilon_L = E_{2,4L}/E_{1L}$	$\epsilon_D = E_{1,3L}/E_{2L}$
$Pe_L = \mu E_{3L} w_L / \kappa$	$Pe_D = \mu E_{4D} w_D / \kappa$	

Table 2 – Cross injector physical variables for loading (a) and dispensing (b) stages. The resulting non-dimensional variables for both stages (c) reduce the number of degrees of freedom from 8 to 5.

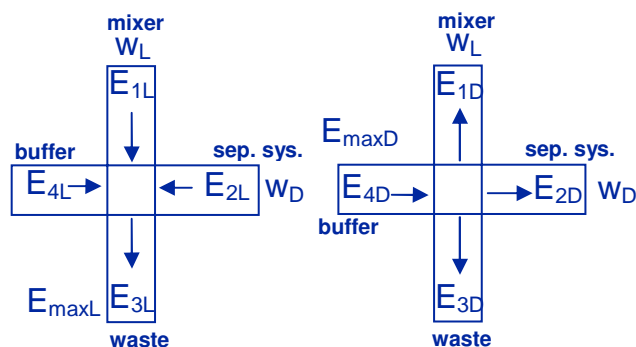


Figure 2 –The general layout of the cross injector with respect to the rest of the separation system for loading and dispensing stages.

obtained using the Buckingham-Pi Theorem [8]. Performance for each stage (loading and dispensing) is determined by 3 dimensionless parameters, the ratio of the channel widths, ω , the ratio of accessory to driving field, ϵ , and the Peclet number, Pe . The Peclet number is based upon the maximum electric field, E_{3L} in the loading stage and E_{4D} in the dispensing stage. The parameters ϵ_L and ϵ_D fix the ratio of accessory fields to driving fields in the respective stages.

In order to define the extent of the injector as a system component, the lengths of the legs of the cross are taken as four times the channel width, $\ell=4w$. This value, based upon numerical experiments, results in containment of the entire injection plug within the leg after injection, and isolates the injection chamber of the cross, within which the non-uniform electric fields are the dominant factor in the shaping of the injection plug.

3.1 Electric Fields

Four electric fields, measured at the injector inlets, are involved in each stage of injection, as seen in Figure 2. For the loading stage, E_{1L} represents the field that moves the fluid into the injection chamber and drives an inward current density. E_{2L} and E_{4L} represent the accessory fields that pinch the analyte fluid in the injection chamber, with inward current densities. For symmetric pinching: $E_{2L}=E_{4L} \equiv E_{2,4L}$. Finally, E_{3L} is the field with the largest magnitude, with an outward current density transporting the tail of the injection plug into the waste reservoir. Conservation of current for a surface that surrounds the injection chamber results in:

$$E_{3L} = E_{1L} + 2 \frac{w_D}{w_L} E_{2,4L} \quad (1)$$

For the dispensing stage, E_{2D} is the driving field that carries the plug into the separation channel and has an outward current density. E_{1D} and E_{3D} are the accessory fields with outward current densities that symmetrically pull the analyte out of the injection chamber, so that $E_{1D}=E_{3D} \equiv E_{1,3D}$. E_{4D} is the dispensing field with the largest

magnitude; it flushes out the injection chamber pushing the plug into the separation channel. Again, conservation of current relates the dispensing stage inlet fields:

$$E_{AD} = E_{2D} + 2 \frac{w_L}{w_D} E_{1,3D} \quad (2)$$

Based upon eqs. 1 and 2, for any specific choice of the width ratio, ω , and field ratio, ε , all fields are determined in terms of the maximum field, E_{3L} or E_{4D} .

Finally, to determine the voltages that are necessary to achieve the desired fields for each stage, a linear system describes the relation between the applied voltage and electric field for any cross injector with legs of length $\ell=4w$. With electric fields normalized to the channel width, w , the linear relationships are:

$$\begin{bmatrix} \Phi_{1L} \\ \Phi_{2L} \\ \Phi_{4L} \end{bmatrix} = \begin{bmatrix} 0.1751 & -0.0604 & -0.0604 \\ -0.0604 & 0.1751 & -0.0543 \\ -0.0604 & -0.0543 & 0.1751 \end{bmatrix}^{-1} \begin{bmatrix} E_{1L} \\ E_{2L} \\ E_{4L} \end{bmatrix} \quad (3)$$

$$\begin{bmatrix} \Phi_{1D} \\ \Phi_{3D} \\ \Phi_{4D} \end{bmatrix} = \begin{bmatrix} 0.1751 & -0.0543 & -0.0604 \\ -0.0543 & 0.1751 & -0.0604 \\ -0.0604 & -0.0604 & 0.1751 \end{bmatrix}^{-1} \begin{bmatrix} E_{1D} \\ E_{3D} \\ E_{4D} \end{bmatrix} \quad (4)$$

where E_{mL} and E_{mD} are the desired field values with appropriate signs, and Φ_{mL} and Φ_{mD} are the resulting voltages to be applied to injector's inlets. The matrix coefficients are determined through numerical solutions of Laplace's equation for conduction problems within the injector. One of the node voltages is a reference ground node in each stage (Φ_{3L} and Φ_{2D}), so that a 3x3 matrix fully describes the relationship between applied voltages and fields. The voltages obtained in eqs. 3 and 4 are used solely for obtaining the fields in the injector. When connected to the rest of the network, these voltages are appropriately biased by the reference node voltage.

3.2 Reduced Problem Space

In order to create a simple analytic model for the output variance and peak concentration, the 5-dimensional parameter space must be considerably reduced. To do this the following assumptions are made:

- The channels widths are the same, $\omega=1$.
- The loading electric field ratio is fixed at $\varepsilon_L=1/2$.
- The dispensing electric field ratio is fixed at $\varepsilon_D=2$.

The majority of designs use channels with the same widths, justifying the first assumption. The second and third assumptions are based on a case study of optimal injector performance at $Pe_L=Pe_D=100$. For this study, numerical experiments were run on an injector with varying

values of ε_L and ε_D . As suggested by Ermakov, the performance was measured by the ratio of the maximum concentration to the standard deviation of the resulting plug after the dispensing stage [5]. This metric gives a measure of the quantity of the analyte injected and how dispersed it becomes. High performance results from large quantity and small dispersion, and reaches a maximum at $\varepsilon_L=0.5$ and $\varepsilon_D=2.0$. This agrees qualitatively with Ermakov's results for his case study at $Pe_L=Pe_D=250$, where he found $\varepsilon_L=0.33$, $\varepsilon_D=1.2$. Both cases suggest that the exit control field ratios should be higher than the pinching field ratios. After w , ε_L , and ε_D are fixed, the remaining non-dimensional parameters are Pe_L and Pe_D .

4 RESULTS

With the reduced parameter space, numerical simulations were run using Femlab for Pe_L and Pe_D ranging from 10 to 5000. Peclet numbers below this range for an injector lead to completely undesirable performance due to the large amount of diffusion that dominates each step. Peclet numbers above this range represent diffusion coefficients below $7 \times 10^{-12} \text{ m}^2/\text{s}$ for fields of 50kV/m and electrokinetic mobilities of $1.4 \times 10^{-8} \text{ m}^2/\text{Vs}$. Therefore, the range of Peclet number from 10 to 5000 encompasses the majority of practical system properties.

Simulations were run at 64 points in the parameter space. After the numerical results were obtained, they were converted to a closed-form analytical expression by fitting the numerical results with a two dimensional polynomial. The order of the polynomial in each dimension was chosen to minimize the error. The result was the product of a 7th order polynomial in $\text{Log}_{10}(Pe_L)$ and $\text{Log}_{10}(Pe_D)$ for describing the normalized variance (σ^2/w^2), and the product of a 6th order polynomial in $\text{Log}_{10}(Pe_L)$ and 7th order polynomial in $\text{Log}_{10}(Pe_D)$ for describing the normalized peak concentration (C_{max}/C_o , where C_o is the input concentration).

Figure 3 shows the plug variance and peak concentration as functions of Pe_L and Pe_D on logarithmic scales. These results indicate that the larger the Peclet numbers become, the better the injector performs. The worst expected performance for this injection scheme is approximately the width of the channel squared. The analytical model has a maximum error of less than 2% based upon the Femlab simulations. After the analytical model has been established through fitting to the numerical simulations, it takes less than ~0.5s to evaluate any point in the space, whereas the numerical simulations take ~4.5hrs per point, yielding a 32,000X increase in speed.

5 SYSTEM LEVEL INTEGRATION

Integration of the injector model with the other component models in a network requires a global determination of the node voltages. This is accomplished

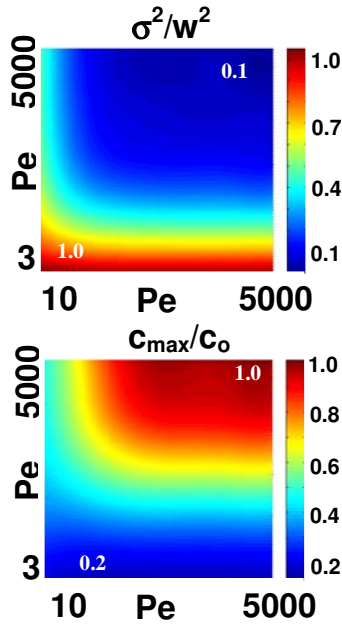


Figure 3 –Results of the injector model in the Pe_L and Pe_D problem space, showing the normalized variance and the normalized peak concentration.

through construction of an equivalent resistor network representing all legs of the system, as seen in Figure 4. The equivalent resistances are:

$$R_{1,3,4} = \frac{L_{1,3,4}}{\sigma w h} \quad (5)$$

$$R_2 = \sum_{i=1}^N \frac{L_{2i}}{\sigma w h} + \sum_{j=1}^M \frac{\theta}{\sigma \ln(r_o / r_i) h}, \quad (6)$$

where $L_{1,3,4}$ are the lengths of the channels connected to the injector, L_{2i} are the lengths of the separation channel segments, σ is the buffer conductance, w is the channel width, h is the channel depth, θ is the turn angle, r_o is the outer turn radius, r_i is the inner turn radius, N is the number of straight segments, and M is the number of turns. Eq. 6, accounts for the radially varying field structure in calculating the resistance of the curved separation channels.

The resulting network is then solved for the global node voltages ($V_{1L}, V_{4L}, V_{oL}, V_{2L}, V_{1D}, V_{4D}, V_{oD}, V_{3D}$), as seen in Figure 4. Then the internal separation channel node voltages are solved using a Kirchoffian linear system with the individual resistances. A complete description of the implementation in VerilogA is provided in [9].

6 CONCLUSION

In this paper a closed-form analytical model of a 2-stage cross injector is developed. The full 5-dimensional parameter space is reduced to only the Peclet numbers in the loading and dispensing stages for given field ratios and constant channel widths. The resulting polynomial fit model is 32,000 times faster than pure numerical simulation, and is integrated into a system network of

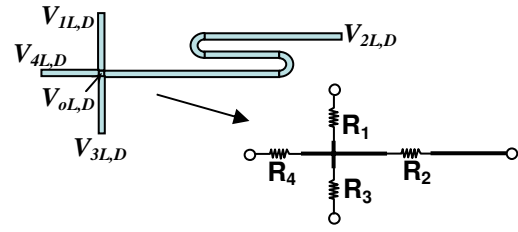


Figure 4 – Equivalent resistor network of injection and separation systems.

component models using the input concentrations and providing the plug variances and peak concentrations as outputs. The model predicts a worst case variance of $\sim w^2$ and has less than 2% maximum error relative to the original PDE solutions. The integration with the rest of the system is completed with a Kirchoffian network analysis to provide voltages for all ports and nodes in the network using equivalent resistor networks.

Future similar models for more complex injector types will permit system network representations of tradeoffs between alternative injector designs in interactions with other system components.

ACKNOWLEDGEMENTS

This research effort is sponsored by the Defense Advanced Research Projects Agency under the Air Force Research Laboratory, Air Force Material Command, USAF, under grant number F30602-01-2-0587 and the NSF ITR program under grant number CCR-0325344. Computing resources were made possible by NSF equipment grant CTS-0094407 and Intel Corporation.

REFERENCES

- [1] Jacobson, S.C; Hergenröder, R.; Koutny, L.B.; et. al., Vol. 66, *Analytical Chemistry* 1994, pp. 1107-1113.
- [2] Ermakov, S.V.; Jacobson, S.C.; Ramsey, J.M., Vol. 70, *Analytical Chemistry* 1998, pp. 4494-4504.
- [3] Shultz-Lockyear, L.L.; Colyer, C.L.; et. al., Vol. 20, *Electrophoresis* 1999, pp. 529-538.
- [4] Deshpande, M.; Greiner, K.B.; West, J.; Gilbert, J.R., *Micro Total Analysis Systems* 2000, pp. 339-342.
- [5] Ermakov, S.V.; Jacobson, S.C.; Ramsey, J.M., Vol. 72, *Analytical Chemistry* 2000, pp. 3512-3517.
- [6] Pfeiffer, A.J.; Mukherjee, T.; Hauan, S., *Proceedings of NanoTech* 2003, pp. 250-253.
- [7] Wang, Y.; Lin, Q.; Mukherjee, T., *MicroTAS* 2003, Oct. 5-9, Squaw Valley, CA, USA.
- [8] Hanche-Olsen, H., "Buckingham's π -Theorem", <http://www.math.ntnu.no/~hanche/notes/buckingham/buckingham-a4.pdf>. 1998
- [9] Wang, Y.; Lin, Q.; Mukherjee, T., *NanoTech* 2004, Mar. 7-11, Boston, MA, USA.